Abdominal Radiology

Published online: 6 July 2018

Abdom Radiol (2019) 44:122–130
https://doi.org/10.1007/s00261-018-1681-2

MRI of pancreatic ductal adenocarcinoma: texture analysis of T2-weighted images for predicting long-term outcome

Moon Hyung Choi,[1,3] Young Joon Lee,[1,3] Seung Bae Yoon,[2,3] Joon-Il Choi,[1,3] Seung Eun Jung,[1,3] and Sung Eun Rha[1]

[1]Department of Radiology, Seoul St. Mary's Hospital, College of Medicine, The Catholic University of Korea, 222 Banpo-daero, Seocho-gu, Seoul 06591, Republic of Korea
[2]Department of Internal Medicine, Seoul St. Mary's Hospital, College of Medicine, The Catholic University of Korea, Seoul, Republic of Korea
[3]Cancer Research Institute, College of Medicine, The Catholic University of Korea, Seoul, Republic of Korea

Abstract

Purpose: To assess the association between T2-weighted imaging (T2WI) texture-analysis parameters and the pathological aggressiveness or long-term outcomes in pancreatic ductal adenocarcinoma (PDAC) patients.
Methods: A total of 66 patients (mean age 65.3 ± 9.0 years) who underwent preoperative MRI followed by pancreatectomy for PDAC between 2013 and 2015 were included in this study. A radiologist performed a texture analysis twice on one axial image using commercial software. Differences in the tex parameters, according to pathological factors, were analyzed using a Student's *t* test or an ANOVA with Tukey's test. Univariate and multivariate Cox proportional hazards regression analyses were used to evaluate the association between tex parameters and recurrence-free survival (RFS) or overall survival (OS).
Results: The mean follow-up time was 18.5 months, and there were 58 recurrences and 39 deaths. The mean of the positive pixel (MPP)-related factors was significantly lower in poorly differentiated tumors than in well-differentiated tumors as well as in cases with perineural invasion. The univariate Cox proportional hazards analysis showed a significant association between the tex parameters and RFS or OS. However, only tumor size was statistically significant after the multivariate analysis. Only tumor size and entropy with medium texture were significantly associated with OS after the multivariate analysis.
Conclusions: Tumor size was a significant predictive factor for RFS and OS in PDAC patients. Although entropy with medium texture analysis was significantly associated with OS, there were also limitations in the texture analysis; thus, further study is necessary.

Key words: Magnetic resonance imaging—Pancreatic neoplasms—Adenocarcinoma—Recurrence

Pancreatic ductal adenocarcinoma (PDAC) is a devastating cancer that has a poor recurrence-free survival (RFS) and overall survival [1]. Surgical resection of pancreatic cancer is the only potential curative treatment. Currently, neoadjuvant chemotherapy, followed by surgical resection, is used for resectable or borderline resectable PDAC [2]. Therefore, preoperative imaging is the most important factor for determining the treatment plan; however, the exact border of the pancreatic cancer is often hard to define [3, 4]. Sensitivity and specificity of a CT/MRI in diagnosing tumor staging are approximately 60 and 96%, respectively [5]. Localized pancreatic cancers on preoperative imaging studies can invade peripancreatic fat or adjacent structures [6–8]. Furthermore, tumor recurrence is frequent, even after radical resection of the pancreatic cancer [9–11].

If preoperative imaging can provide information about prognosis of the patient, as well as resectability, it will be more useful to determine how to treat patients. Moreover, as several pathological factors, such as surgical margin and perineural/vascular invasion, have been shown to be associated with the prognosis of patients, correlation of radiologic finding to aggressive pathologic

Electronic supplementary material The online version of this article (https://doi.org/10.1007/s00261-018-1681-2) contains supplementary material, which is available to authorized users.

Correspondence to: Young Joon Lee; *email:* yjleerad@catholic.ac.kr

features can drive a more aggressive treatment [12]. Several studies showed that some CT findings of PDAC were prognostic factors for patient outcome [13, 14]. A recent study reported that rim enhancement on an MRI was associated with poor patient outcome [15]. Similar to the semantic features of preoperative imaging, quantitative parameters may also predict patient outcome.

Among many quantitative imaging analyses, CT texture analysis has been correlated with pathological results and has been used to predict the outcomes of PDAC patients in a few studies [16, 17]. These studies suggest that some tex parameters can be biomarkers for aggressive tumor pathology and poor patient outcomes. Texture analysis can be used as a tool to assess tumor heterogeneity, and we can acquire information about the arrangement of pixels in a selected area [18, 19]. However, MRI-based texture analysis has not been performed in PDAC. Texture analysis of T2-weighted imaging (T2WI) from MRI has been used in many cancers, including breast, prostate, endometrial, and rectal cancer [20–25]. Despite potential variability in T2-signal intensity, a previous study reported high reproducible results of tex features from three different MRI imaging scanners [26, 27]. As an MRI has a superior soft tissue contrast compared to CT, we expect that the T2-signal intensity will reflect the composition of PDAC and that the MR-texture analysis will show potential as a biomarker to predict patient outcome.

The purpose of this study was to assess the association between T2-weighted imaging (T2WI) tex parameters and the pathological aggressiveness or long-term outcomes in PDAC patients.

Materials and methods

This study was approved by the institutional review board, and the informed consent requirement was waived due to the retrospective study design.

Patients

Consecutive patients who underwent any type of pancreatectomy for a pancreatic tumor between January 2013 and December 2015 were eligible for this study. The inclusion criteria were as follows: (1) preoperative MRI performed in our institution before pancreatectomy and (2) a diagnosis of PDAC that was pathologically confirmed after pancreatectomy. Pancreatectomy was defined as one of the following: Whipple's operation, pylorus-preserving pancreaticoduodenectomy, distal pancreatectomy, or total pancreatectomy. The exclusion criteria were as follows: (1) pancreatic tumor, other than PDAC, such as benign tumor or intraductal papillary mucinous neoplasm with an associated invasive carcinoma; (2) preoperative MRI was performed at another institution; and (3) preoperative MRI had not been performed within 50 days prior to the pancreatectomy. Finally, 68 patients were enrolled in this study. A flowchart showing the number of patients who were included or excluded is presented in Fig. 1. Age, sex, and preoperative laboratory findings were collected from the electronic medical records.

Image analysis

All the preoperative MRIs were performed using a 3-T MRI machine (Magnetom Verio, Siemens Healthcare, Erlangen, Germany). Fat-suppressed, turbo-spin-echo T2WI with respiratory triggering (repetition time, 4000–5400 ms; echo time, 100–123 ms; echo train length, 21; thickness, 6 mm; slice gap, 0; field of view, 380 × 309 mm; matrix size, 448 × 255; number of excitations, 2; acquisition time, 4 min 30 s) was used for image analysis. Image analysis was performed twice in a 2 week interval by one abdominal radiologist with 8 years of experience using the commercial tex software (TexRAD Ltd, Somerset, UK). She knew that the patients had underwent pancreatectomy and that pancreatic tumors were pathologically confirmed as PDAC, but other clinical information, such as recurrence-free survival or overall survival, were not made known to her. The radiologist selected a single axial T2WI that contained the tumor with the largest diameter and drew a region-of-interest (ROI) around the entire area of the pancreatic cancer using the polygon ROI tool (Fig. 2). As the dedicated software did not provide a volumetric analysis, we performed texture analysis on a single axial slice. PDAC was defined as the area that had a slightly higher signal intensity than the pancreatic parenchyma on the T2WI. Although only the T2WI was used for image analysis, the radiologist could review other sequences from the MRI to determine the border of the tumor. If a focal area with signal intensity similar to water was in the PDAC, the area was considered to be necrotic or a cystic change in the tumor and was included

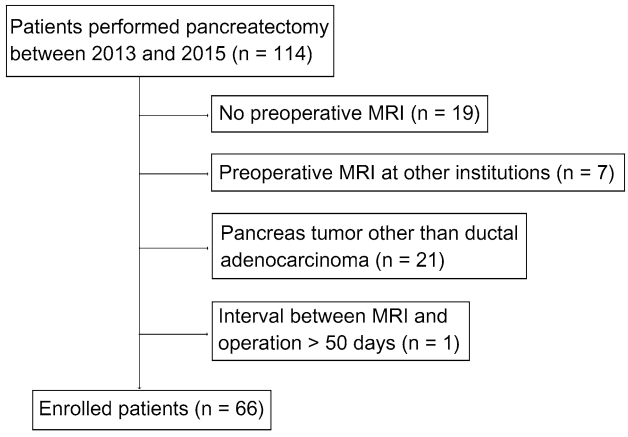

Fig. 1. Flowchart showing the selection process for the study population.

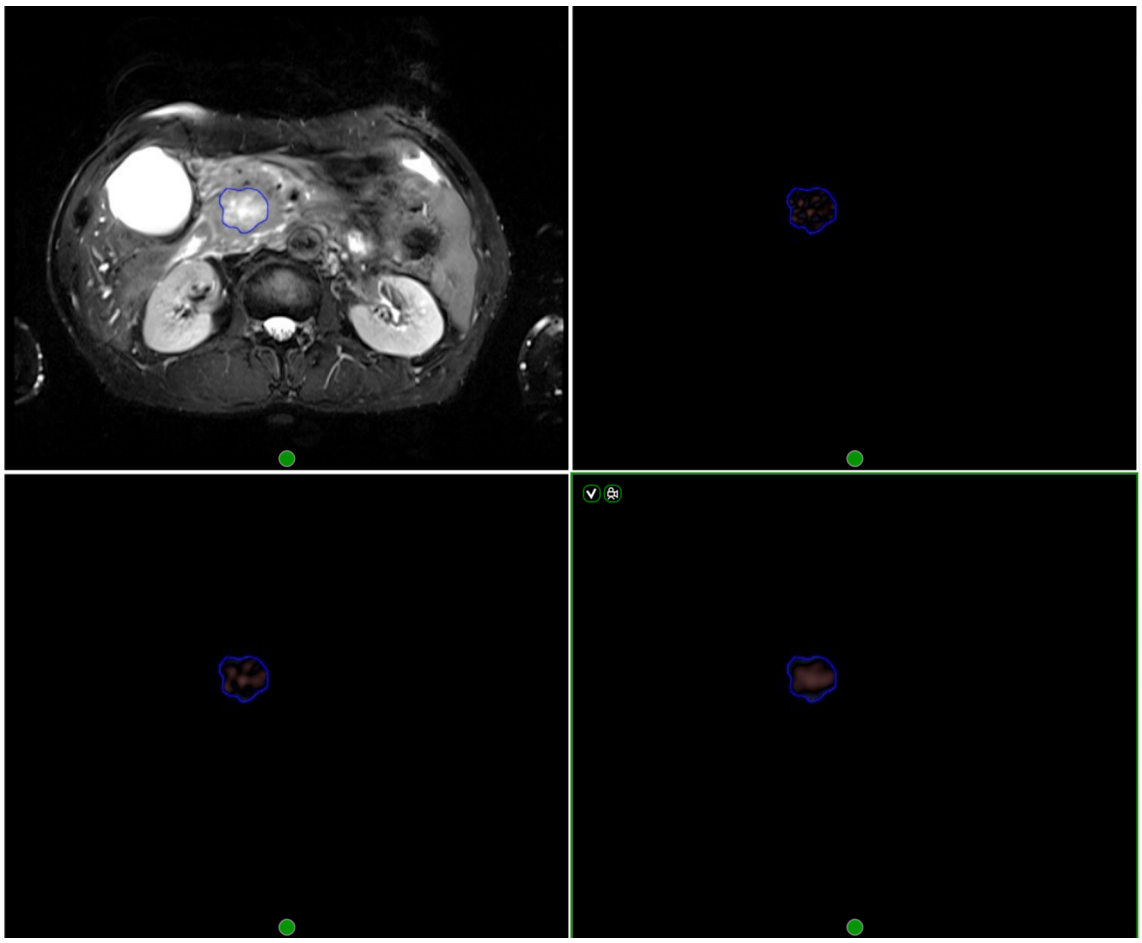

Fig. 2. An example of texture analysis of pancreatic ductal adenocarcinoma using different filter levels (spatial scaling factors 2, 4, and 6) in a 66-year-old male.

in the ROI. In contrast, if the cystic lesion was not continuous to the PDAC, this area was considered a pseudocyst and was not included in the ROI. The dedicated software performed filtration of the pixels in the ROI at first and then texture analysis. Filtration can be performed using six levels of spatial scaling factor (SSF), from fine to coarse texture. An SSF 0 meant the absence of filtration. An SSF 2 highlighted fine texture features, which were 2 mm in radius. An SSF 3 or 4 (medium) and an SSF 5 or 6 (coarse) highlighted texture features which were 3, 4, 5, or 6 mm in radius, respectively. The software provided six texture-analysis parameters at each SSF, including the mean and standard deviation (SD) of pixel signal intensity, skewness (asymmetry) and kurtosis (peakedness) of the pixel signal intensity histogram, entropy (irregularity of gray-level distribution), and mean of the positive pixels (MPP, mean signal intensity of pixels with a signal intensity greater than 0).

Pathological results

Pathological assessments were made after pancreatectomy by a pathologist with 20 years of experience in the pancreaticobiliary system. Tumor size, location, differentiation, resection margin (R0 or R1), lymphatic invasion, microvascular invasion, and perineural invasion were reported. The TNM stage according to the AJCC 7th edition was also reported.

Patient outcomes

RFS and OS were evaluated in this study. RFS was measured from the date of surgery to the date of the radiological examination, during which the recurrence was initially found. For patients without recurrence, the interval from the date of surgery to the date of the last clinical follow-up was measured as the RFS. OS was defined as the interval between the date of surgery to the date of death for expired patients and to the date of last outpatient follow-up for live patients.

Statistical analysis

Differences in texture-analysis parameters according to pathological characteristics were analyzed using independent t tests or one-way ANOVAs followed by Tu-

key's post hoc tests. As there was only one patient with a TNM stage of III, differences in parameters among the TNM stages were only evaluated for stages I and II. An intraobserver agreement was evaluated using an intraclass correlation coefficient (ICC). The ICC was interpreted as follows: ≤ 0.20, slight agreement; 0.20–0.40, fair agreement; 0.41–0.60, moderate agreement; 0.61–0.80, substantial agreement; > 0.80, almost perfect agreement. A Cox proportional hazards regression was used to find statistically significant factors for predicting RFS and OS. Any factors with a *P*-value of < 0.05 on univariate analysis were included in a multivariate analysis. For statistically significant factors that remained after the multivariate analysis, we searched the best cutoff values to discriminate poor and good long-term outcomes, using the maximal Chi-squared method. RFS or OS were determined using the Kaplan–Meier method, and the differences among the groups were compared by the logrank test. All statistical analyses were performed using SPSS version 24 (IBM Corporation, Armonk, NY, USA) and the Moon's R website (http://web-r.org). A *P*-value of < 0.05 was considered statistically significant.

Results

The mean age of the 66 patients in this study was 65.3 ± 9.0 years old (range 36–84 years). Most cancers were located in the head of the pancreas (78.8%), and the mean tumor size was 3.7 ± 1.8 cm. The resection margin was positive in 27 patients. The baseline characteristics of the patients are summarized in Table 1. There were 58 recurrences and 39 deaths. The mean time to recurrence was 10.7 months (range 0.7–51.9 months). Recurrent cancers were detected at operation site (n = 20), liver (n = 14), lung (n = 6), peritoneum (n = 8), lymph node (n = 3), and multiple organs (n = 4). Recurrent sites of three patients were not recorded. The mean OS was 18.5 months (range 1.4–55.4 months). No patient underwent radiotherapy or chemotherapy before surgery. After surgery, 56 patients (84.8%) underwent adjuvant chemotherapy.

Most parameters, from fine to coarse filtration levels, showed substantial to almost perfect intraobserver agreement (Table 2). The ICC of the mean value and SD tended to decrease as the SSF value increased. Skewness and kurtosis showed higher ICCs at the coarser filtration levels. Entropy and MPP showed almost perfect agreement consistently, regardless of the filter size used.

Many texture-analysis parameters were significantly different, according to each pathological factor. Table 3 shows the mean values of significantly different variables from the second set of image analysis, according to pathological factors. Mean SD and MPP, from fine-to-coarse texture, were significantly different according to

Table 1. Baseline characteristics

	Study population (n = 66)
Male sex	30 (45.5)
Age (years)	65.3 ± 9.0 (36–84)
CA 19–9 (U/mL)	507.1 ± 1063.3 (2.5–7200.0)
Tumor size (cm)	3.7 ± 1.8 (1.4–11.5)
Location of tumor	
Head	52 (78.8)
Body and tail	14 (21.2)
Operation	
Whipple's operation	12 (18.2)
Pylorus preserving pancreaticoduodenectomy	39 (59.1)
Distal pancreatectomy	11 (16.7)
Total pancreatectomy	4 (6.1)
Adjuvant chemotherapy after surgery	
Performed	56 (84.8)
Not performed	10 (15.2)
TNM stage	
Stage IB	3 (4.5)
Stage IIA	17(25.8)
Stage IIB	45 (68.2)
Stage III	1 (1.5)
Differentiation	
Poorly differentiated	10 (15.2)
Moderately differentiated	46 (69.7)
Well-differentiated	10 (15.2)
Resection margin	
Negative (R0 resection)	39 (59.1)
Positive (R1 resection)	27 (40.9)
Lymphatic invasion	
Negative	19 (28.8)
Positive	47 (71.2)
Vascular invasion	
Negative	29 (43.9)
Positive	37 (56.1)
Perineural invasion	
Negative	4 (6.1)
Positive	62 (93.9)

Results are expressed as numbers (percentages) for categorical variables and means ± standard deviations (ranges) for quantitative variables

Table 2. Intraobserver agreement for texture-analysis variables

Variables	ICC	*P*-value	Variables	ICC	*P*-value
SSF 0			SSF 4		
Mean	0.950	< 0.001	Mean	0.400	< 0.001
SD	0.888	< 0.001	SD	0.752	< 0.001
Entropy	0.891	< 0.001	Entropy	0.908	< 0.001
MPP	0.950	< 0.001	MPP	0.891	< 0.001
Skewness	0.451	0.008	Skewness	0.662	< 0.001
Kurtosis	0.192	0.196	Kurtosis	0.715	< 0.001
SSF 2			SSF 5		
Mean	0.705	< 0.001	Mean	0.384	0.026
SD	0.861	< 0.001	SD	0.718	< 0.001
Entropy	0.895	< 0.001	Entropy	0.903	< 0.001
MPP	0.934	< 0.001	MPP	0.893	< 0.001
Skewness	0.512	0.002	Skewness	0.720	< 0.001
Kurtosis	0.374	0.031	Kurtosis	0.620	< 0.001
SSF 3			SSF 6		
Mean	0.501	0.003	Mean	0.419	0.015
SD	0.802	< 0.001	SD	0.718	< 0.001
Entropy	0.895	< 0.001	Entropy	0.893	< 0.001
MPP	0.911	< 0.001	MPP	0.906	< 0.001
Skewness	0.574	< 0.001	Skewness	0.769	< 0.001
Kurtosis	0.626	< 0.001	Kurtosis	0.640	< 0.001

Table 3. Mean values of significantly different variables from the second texture analysis according to pathological factors

Texture analysis	Pathologic factors			*P*-value
	Differentiation			
	Poorly differentiated	Moderately differentiated	Well-differentiated	
Mean (SSF0)	249.4 ± 103.1	285.8 ± 88.9	390.6 ± 275.5	0.047
Mean (SSF2)	6.3 ± 26.7[a]	26.5 ± 27.8	49.8 ± 72.9[a]	0.041
SD (SSF0)	49.7 ± 13.9	46.7 ± 18.8[a]	84.4 ± 89.8[a]	0.021
SD (SSF2)	143.1 ± 59.4	130.4 ± 46.9[a]	223.8 ± 216.2[a]	0.021
SD (SSF6)	159.5 ± 49.8	149.4 ± 52.0	255.8 ± 257.1	0.023
MPP (SSF0)	249.4 ± 103.1	285.8 ± 88.9	390.6 ± 275.5	0.047
MPP (SSF2)	106.7 ± 45.6[a]	113.1 ± 40.8	200.2 ± 200.0[a]	0.014
MPP (SSF3)	124.7 ± 50.6[a]	139.6 ± 51.0	219.9 ± 215.1[a]	0.039
MPP (SSF4)	142.4 ± 60.0[a]	161.5 ± 58.6	251.7 ± 233.5[a]	0.033
MPP (SSF5)	170.7 ± 81.7[a]	181.0 ± 66.5	299.5 ± 272.6[a]	0.019
MPP (SSF6)	189.7 ± 95.2[a]	204.0 ± 78.2	346.1 ± 317.0[a]	0.015

	Resection margin		*P*-value
	Negative	Positive	
SD (SSF5)	188.4 ± 126.7	136.8 ± 41.5	0.046

	Vascular invasion		*P*-value
	Negative	Positive	
Skewness (SSF2)	0.45 ± 0.47	0.08 ± 0.58	0.007
Skewness (SSF3)	0.33 ± 0.57	0.06 ± 0.50	0.043
Skewness (SSF6)	0.21 ± 0.53	− 0.09 ± 0.56	0.034

	Perineural invasion		*P*-value
	Negative	Positive	
Mean (SSF0)	476.0 ± 365.6	284.6 ± 10.80	0.006
SD (SSF0)	101.9 ± 118.7	49.7 ± 28.5	0.010
SD (SSF2)	272.5 ± 270.4	138.3 ± 74.3	0.007
SD (SSF3)	282.7 ± 276.0	152.4 ± 76.7	0.010
SD (SSF4)	295.1 ± 284.4	157.5 ± 71.7	0.006
SD (SSF5)	324.2 ± 332.9	157.2 ± 67.8	0.001
SD (SSF6)	350.5 ± 370.9	155.2 ± 67.4	0.001
MPP (SSF0)	476.0 ± 365.6	284.6 ± 108.0	
MPP (SSF2)	232.7 ± 229.8	118.4 ± 71.6	0.012
MPP (SSF3)	244.1 ± 223.0	143.4 ± 82.9	0.044
MPP (SSF4)	279.1 ± 245.2	165.3 ± 92.8	0.040
MPP (SSF5)	341.9 ± 309.1	188.1 ± 105.3	0.018
MPP (SSF6)	392.4 ± 360.8	212.5 ± 123.3	0.018

[a]Significant difference in a post hoc test

differentiation of tumor and perineural invasion. The results of the first set of image analysis and the insignificant factors from the second analysis are summarized in the Supplementary material, 1–3.

There were several parameters that were significantly associated with RFS on the univariate Cox proportional hazards analysis (Table 4, Supplementary material 4). Among the clinical factors, tumor size was associated RFS, with a hazard ratio of 1.278. Results from the first and second sets of image analysis were different. In the first analysis, entropy-related factors were associated with RFS. However, in the second analysis, skewness (SSF2) and kurtosis (SSF3, 4) were associated with RFS. On the multivariate analysis, only tumor size was significantly associated with RFS in both sets of image analysis (Table 4).

Several parameters showed a significant association with OS in the univariate analysis (Table 5, Supplementary material 5). Although SD (SSF2) and MPP (SSF2) from both sets of the image analyses commonly showed significant association in the univariate analysis, they did not remain significant factors after the multivariate analysis. Only entropy (SSF4) in the first set of image analyses was significantly associated, with a 4.347 hazard ratio, even after multivariate analysis (Table 5). The Kaplan–Meier plot showed a discriminatory ability

Table 4. Univariate and multivariate Cox hazard analysis for recurrence-free survival

Variables	Univariate analysis		Multivariate analysis	
	HR	*P*-value	HR	*P*-value
First set of image analysis				
Tumor size	1.278	< 0.001	1.257	0.002
Entropy (SSF3)	1.995	0.049[a]	–	–
Entropy (SSF4)	2.119	0.032[a]	–	–
Entropy (SSF5)	2.153	0.029[a]	–	–
Entropy (SSF6)	2.129	0.025	1.582	0.792–3.162
Second set of image analysis				
Tumor size	1.278	< 0.001	1.246	0.002
Skewness (SSF2)	0.589	0.023	0.704	0.166
Kurtosis (SSF3)	0.767	0.043[a]	–	–
Kurtosis (SSF4)	0.663	0.015	0.737	0.074

HR, hazard ratio; SD, standard deviation; MPP, The mean of the positive pixels
[a]Variables not entered into the multivariate analysis due to strong multicollinearity

Table 5. Univariate and multivariate Cox hazard analysis for overall survival

Variables	Univariate analysis		Multivariate analysis	
	HR	*P*-value	HR	*P*-value
First set of image analysis				
Tumor size	1.341	0.004	1.389	< 0.001
SD (SSF2)	0.993	0.024	0.998	0.782
MPP (SSF2)	0.991	0.027	0.997	0.657
SD (SSF3)	0.995	0.036	–	–
Entropy (SSF4)	2.388	0.045	4.347	0.002
Second set of image analysis				
Tumor size	1.341	0.004	1.459	< 0.001
SD (SSF2)	0.992	0.036	0.984	0.266
MPP (SSF2)	0.989	0.028	1.018	0.326
Mean (SSF5)	0.995	0.031	0.997	0.330
MPP (SSF5)	0.995	0.048	–	–
Mean (SSF6)	0.996	0.026	–	–

HR, hazard ratio; SD, standard deviation; MPP, The mean of the positive pixels
[a]Variables not entered into the multivariate analysis due to strong multicollinearity

between the two groups, divided by the best cutoff of entropy (SSF4) ($P < 0.001$) (Fig. 3).

Discussion

Our study showed that entropy of medium texture from the T2WI texture analysis was significantly associated with the overall survival of PDAC patients after surgery. However, other texture-analysis parameters, which showed statistical significance to predict RFS or OS according to the univariate analysis, did not remain significant after the multivariate analysis. Tumor size was a significant predictive factor for both RFS and OS. Although intraobserver agreement between the two sets of image analyses showed substantial to almost perfect agreement for all the texture-analysis parameters, associations between the texture-analysis parameters and the long-term outcome were different from both sets of image analyses.

In this study, entropy (SSF4) from the first set of image analyses was significantly associated with OS. The cutoff value of entropy (SSF4) could discriminate patients with poor and good OS, and tumors with entropy (SSF4) of 5.62 or less showed significantly longer OS than others. This result may be interpreted as the fact that PDAC has a more random distribution of pixels on T2WIs in the patients with poor OS than those with good OS. Therefore, PDAC with inhomogeneous internal signal intensity may have a poorer prognosis. Other parameters such as the mean, SD or MPP were not significantly associated with RFS or OS. These can be acquired by simple measurement. However, they cannot reflect the arrangement of signal intensities, but generally show the characteristics of the tumor. Therefore, texture analysis may provide more information than simple measurement. A previous study performed in breast cancer showed that entropy of T2WI was related to RFS [22]. In another similar study on prostate cancer, entropy-related factors were associated with biochemical recurrence after prostatectomy [20]. Similar to the results seen with other cancers, our study suggests the possibility of texture analysis as a quantitative method to predict prognosis of PDAC.

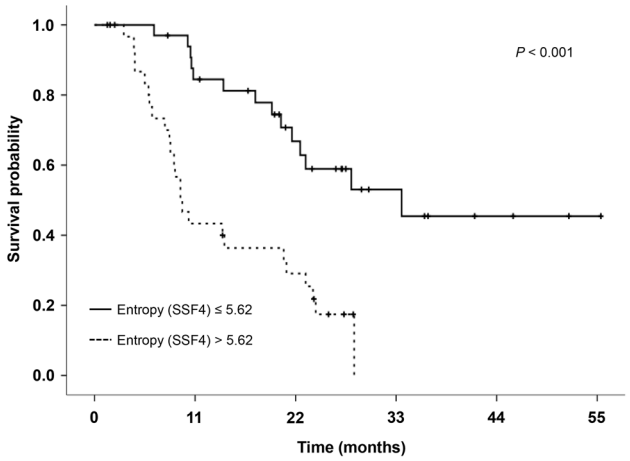

Fig. 3. Overall survival curves after the operation according to entropy (spatial scaling factor 4).

Although tumor size, entropy-, kurtosis- and skewness-related factors showed significant association with RFS on the univariate Cox analysis, only tumor size remained a significant predictive factor after the multivariate Cox analysis. In the results of this study, higher entropy was related to poorer long-term outcomes on the univariate analysis. However, multivariate analysis eliminated the significance of entropy. This finding could be explained by the fact that entropy was higher in the larger tumor and the larger tumor had a higher change of heterogeneous internal signal intensity due to necrosis. A previous study showed that larger tumor size and rim enhancement were independent prognostic factors for lower RFS and OS in pancreatic cancer after surgery [15]. In the same previous study, PDAC with rim enhancement showed a significantly higher rate of necrosis within tumors than others. In this study, we expected that texture-analysis parameters could reflect the necrosis within the tumor. However, the multivariate analysis could not reveal the significance of texture-analysis parameters. The reason for such a result may be that we did not perform volumetric analysis or that we included too small a number of patients to provide the statistical power.

A previous study evaluated the association between the texture analysis of PDAC on CT and RFS; ROIs were drawn around the entire tumor and the central hypo-attenuating area [16]. In the same previous study, lower mean density of the central hypo-attenuating area was significantly associated with poorer RFS. A low-density area on the contrast-enhanced CT may have been a finding of tumor necrosis, which has been related to poor postoperative outcomes in PDAC [28]. In this study, we evaluated T2WI of PDAC. T2WI alone may not be able to reflect the area of necrosis in tumors, but we expected that T2 signal intensity varies depending on the tissue component. Unlike the previous study, we did not draw ROIs for distinguishable areas in the tumor, but for the entire tumor. We found that ROIs for entire tumor analysis seemed to be easier to draw and more objective than selecting focal low-density areas in the tumor, because drawing ROIs for focal areas in the tumor could be subject to the various biases of the radiologist who draws the ROI.

This study showed that many texture-analysis parameters were significantly different according to the pathological findings. Well-differentiated tumors showed significantly higher mean and MPP values than poorly differentiated tumors. MPP was lower in PDAC without perineural invasion than in PDAC with perineural invasion. Therefore, lower T2 signal intensity of PDAC seems to be related to more aggressive tumors, represented by poor differentiation and perineural invasion. A larger standard deviation was noted in well-differentiated tumors, in tumors without perineural invasion and in tumors that had negative resection margins compared to the other tumors. Therefore, less aggressive tumors may have variable signal intensities that are farther away from the mean. Pathologically, well-differentiated PDAC forms glandular structures with abundant mucin production. In contrast, poorly differentiated PDAC has nonglandular solid nests with scanty mucin [29]. As well-differentiated PDAC has more variable components, such as mucin and glandular structures, than poorly differentiated PDAC, it may be reflected as a wider range of T2WI SI in well-differentiated PDAC than in poorly differentiated PDAC. A previous study using CT texture analysis of PDAC showed similar results: mean CT attenuation was negatively associated with a poorly differentiated grade, and SD, entropy, and MPP showed significant associations with perineural invasion [16]. The previous study and our study may suggest the usefulness of texture analysis for quantitative markers associated with pathological characteristics of PDAC.

In this study, almost perfect intraobserver agreement was noted in many texture-analysis parameters. The commercial software that was used in this study provided a simple analytical method, and there may be a low probability of variation between image analyses. However, Cox proportional hazards analysis showed different results between the first and second sets of image analyses. Thus, the factors significantly associated with RFS and OS were different between the results of the two image analyses. These different results suggest that small differences in the texture-analysis parameters could impact the analysis with regards to clinical outcomes. However, it was very encouraging to observe that entropy-related factors from both image analyses were consistently associated with early recurrence. Statistically, type 1 error from multiple hypotheses in a limited number of cases could have occurred in this study [30]. As the number of surgically resected pancreatic cancer was limited, we could not validate our results in other

cases. Further study with more patients will solve the problem.

There were several limitations to this study. First, a small number of patients were included. This study was conducted in a single medical center and included only resected PDAC. As a large proportion of patients with PDAC were diagnosed at the unresectable state, only a small number of patients ultimately underwent surgery. However, we thought that a relatively homogeneous patient group consisting of individuals with resectable PDAC was likely to help reduce the variability of the results. Second, we performed texture analysis by only one radiologist. We could evaluate only intraobserver agreement, but not interobserver agreement. As this study showed a potential for texture analysis as a predictive marker for PDAC, further study with multiple readers is necessary. Third, we did not perform texture analysis on apparent diffusion coefficient (ADC) maps or contrast-enhanced MRI. ADC map derived from diffusion-weighted imaging (DWI) is a well-known functional imaging modality that can reflect tissue characteristics [31]. However, DWI and ADC maps have low spatial resolutions, and we were concerned that actual tumor area would not be properly labeled using these techniques. Although contrast-enhanced MRI could provide information about the vascularity of the tumor, the scan times could vary among patients. This study is a preliminary study to explore the possibility of using texture analysis of MRI for obtaining quantitative markers of PDAC, so we wanted to minimize the variations that could affect our test results.

In conclusion, tumor size was a significant predictive factor for RFS and OS in PDAC patients. Although entropy with medium texture analysis was significantly associated with OS, there were also limitations in the texture analysis; thus, further study is necessary.

Compliance with ethical standards

Funding This study was not funded.

Conflict of interest The authors declare that they have no conflict of interest.

References

1. Conlon KC, Klimstra DS, Brennan MF (1996) Long-term survival after curative resection for pancreatic ductal adenocarcinoma. Clinicopathologic analysis of 5-year survivors. Ann Surg 223:273–279
2. National Comprehensive Cancer Network. Clinical practice guidelines in oncology (NCCN Guidelines). Pancreatic adenocarcinoma. Version 1. 2018. https://www.nccn.org/professionals/physician_gls/pdf/pancreatic.pdf.
3. Hall WA, Mikell JL, Mittal P, et al. (2013) Tumor size on abdominal MRI versus pathologic specimen in resected pancreatic adenocarcinoma: implications for radiation treatment planning. Int J Radiat Oncol Biol Phys 86:102–107. https://doi.org/10.1016/j.ijrobp.2012.11.019
4. Aoki K, Okada S, Moriyama N, et al. (1994) Accuracy of computed tomography in determining pancreatic cancer tumor size. Jpn J Clin Oncol 24:85–87
5. Treadwell JR, Zafar HM, Mitchell MD, et al. (2016) Imaging tests for the diagnosis and staging of pancreatic adenocarcinoma: a meta-analysis. Pancreas 45:789–795. https://doi.org/10.1097/MPA.0000000000000524
6. Shah D, Fisher WE, Hodges SE, et al. (2008) Preoperative prediction of complete resection in pancreatic cancer. J Surg Res 147:216–220. https://doi.org/10.1016/j.jss.2008.02.061
7. Porembka MR, Hawkins WG, Linehan DC, et al. (2011) Radiologic and intraoperative detection of need for mesenteric vein resection in patients with adenocarcinoma of the head of the pancreas. HPB (Oxford) 13:633–642. https://doi.org/10.1111/j.1477-2574.2011.00343.x
8. Allen VB, Gurusamy KS, Takwoingi Y, et al. (2016) Diagnostic accuracy of laparoscopy following computed tomography (CT) scanning for assessing the resectability with curative intent in pancreatic and periampullary cancer. Cochrane Database Syst Rev 7:CD009323. https://doi.org/10.1002/14651858.CD009323.pub3
9. Van den Broeck A, Sergeant G, Ectors N, et al. (2009) Patterns of recurrence after curative resection of pancreatic ductal adenocarcinoma. Eur J Surg Oncol 35:600–604. https://doi.org/10.1016/j.ejso.2008.12.006
10. Yamamoto T, Yagi S, Kinoshita H, et al. (2015) Long-term survival after resection of pancreatic cancer: a single-center retrospective analysis. World J Gastroenterol 21:262–268. https://doi.org/10.3748/wjg.v21.i1.262
11. Shimada K, Sakamoto Y, Nara S, et al. (2010) Analysis of 5-year survivors after a macroscopic curative pancreatectomy for invasive ductal adenocarcinoma. World J Surg 34:1908–1915. https://doi.org/10.1007/s00268-010-0570-9
12. Bilici A (2014) Prognostic factors related with survival in patients with pancreatic adenocarcinoma. World J Gastroenterol 20:10802–10812. https://doi.org/10.3748/wjg.v20.i31.10802
13. Fukukura Y, Takumi K, Higashi M, et al. (2014) Contrast-enhanced CT and diffusion-weighted MR imaging: performance as a prognostic factor in patients with pancreatic ductal adenocarcinoma. Eur J Radiol 83:612–619. https://doi.org/10.1016/j.ejrad.2013.12.016
14. Kim JH, Park SH, Yu ES, et al. (2010) Visually isoattenuating pancreatic adenocarcinoma at dynamic-enhanced CT: frequency, clinical and pathologic characteristics, and diagnosis at imaging examinations. Radiology 257:87–96. https://doi.org/10.1148/radiol.10100015
15. Lee S, Kim SH, Park HK, et al. (2018) Pancreatic ductal adenocarcinoma: rim enhancement at MR imaging predicts prognosis after curative resection. Radiology . https://doi.org/10.1148/radiol.2018172331
16. Cassinotto C, Chong J, Zogopoulos G, et al. (2017) Resectable pancreatic adenocarcinoma: role of CT quantitative imaging biomarkers for predicting pathology and patient outcomes. Eur J Radiol 90:152–158. https://doi.org/10.1016/j.ejrad.2017.02.033
17. Eilaghi A, Baig S, Zhang Y, et al. (2017) CT texture features are associated with overall survival in pancreatic ductal adenocarcinoma—a quantitative analysis. BMC Med Imaging 17:38. https://doi.org/10.1186/s12880-017-0209-5
18. Castellano G, Bonilha L, Li LM, et al. (2004) Texture analysis of medical images. Clin Radiol 59:1061–1069. https://doi.org/10.1016/j.crad.2004.07.008
19. Lubner MG, Smith AD, Sandrasegaran K, et al. (2017) CT texture analysis: definitions, applications, biologic correlates, and challenges. Radiographics 37:1483–1503. https://doi.org/10.1148/rg.2017170056
20. Gnep K, Fargeas A, Gutierrez-Carvajal RE, et al. (2017) Haralick textural features on T2-weighted MRI are associated with biochemical recurrence following radiotherapy for peripheral zone prostate cancer. J Magn Reson Imaging 45:103–117. https://doi.org/10.1002/jmri.25335
21. Niu XK, Chen ZF, Chen L, et al. (2017) Clinical application of biparametric MRI texture analysis for detection and evaluation of high-grade prostate cancer in zone-specific regions. AJR Am J Roentgenol . https://doi.org/10.2214/AJR.17.18494
22. Kim JH, Ko ES, Lim Y, et al. (2017) Breast cancer heterogeneity: MR imaging texture analysis and survival outcomes. Radiology 282:665–675. https://doi.org/10.1148/radiol.2016160261

23. Ueno Y, Forghani B, Forghani R, et al. (2017) Endometrial carcinoma: MR imaging-based texture model for preoperative risk stratification-A preliminary analysis. Radiology. 284:748–757. https://doi.org/10.1148/radiol.2017161950
24. Jalil O, Afaq A, Ganeshan B, et al. (2017) Magnetic resonance based texture parameters as potential imaging biomarkers for predicting long-term survival in locally advanced rectal cancer treated by chemoradiotherapy. Colorectal Dis 19:349–362. https://doi.org/10.1111/codi.13496
25. De Cecco CN, Ganeshan B, Ciolina M, et al. (2015) Texture analysis as imaging biomarker of tumoral response to neoadjuvant chemoradiotherapy in rectal cancer patients studied with 3-T magnetic resonance. Invest Radiol 50:239–245. https://doi.org/10.1097/RLI.0000000000000116
26. Kassner A, Thornhill RE (2010) Texture analysis: a review of neurologic MR imaging applications. AJNR Am J Neuroradiol 31:809–816. https://doi.org/10.3174/ajnr.A2061
27. Herlidou-Meme S, Constans JM, Carsin B, et al. (2003) MRI texture analysis on texture test objects, normal brain and intracranial tumors. Magn Reson Imaging 21:989–993
28. Hiraoka N, Ino Y, Sekine S, et al. (2010) Tumour necrosis is a postoperative prognostic marker for pancreatic cancer patients with a high interobserver reproducibility in histological evaluation. Br J Cancer 103:1057–1065. https://doi.org/10.1038/sj.bjc.6605854
29. Luttges J, Schemm S, Vogel I, et al. (2000) The grade of pancreatic ductal carcinoma is an independent prognostic factor and is superior to the immunohistochemical assessment of proliferation. J Pathol 191:154–161
30. Chalkidou A, O'Doherty MJ, Marsden PK (2015) False discovery rates in PET and CT studies with texture features: a systematic review. PLoS One 10:e0124165. https://doi.org/10.1371/journal.pone.0124165
31. Koh DM, Collins DJ (2007) Diffusion-weighted MRI in the body: applications and challenges in oncology. AJR Am J Roentgenol 188:1622–1635. https://doi.org/10.2214/AJR.06.1403